

# Study of Tribology over the Past Twenty Years –Fundamentals and Applications–



**Professor Koji KATO**

Department of Mechanical Engineering,  
College of Engineering, Nihon University

*The representative research results over the past 20 years at my laboratory are introduced as follows,*

- (1) *Static friction coefficient changes by the shape of contact area.*
- (2) *Different wear modes are classified in one diagram as Wear Map by introducing indexes of severity of contact.*
- (3) *Repeated sliding friction at self-mated SiC and Si<sub>3</sub>N<sub>4</sub> in water generates friction coefficient below 0.01.*  
*Micro texture on contact surfaces generates friction coefficient in the order of 0.0001.*
- (4) *Tribo-coating of indium on the surface of SUS440C disk generates friction coefficient below 0.05 against Si<sub>3</sub>N<sub>4</sub> pin in high vacuum.*
- (5) *N<sub>2</sub> gas supply at the contacts of Si<sub>3</sub>N<sub>4</sub>/CNx and CNx/CNx in air generates friction coefficient in the order of 0.001.*
- (6) *Tribolayer formed by tribo-chemical reaction changes friction and wear drastically.*

**Key Words:** *micro-slip, wear map, water lubrication, tribo-coating, N<sub>2</sub>-gas lubrication, tribolayer*

## 1. Introduction

Tribology, a field whose name derives from the Greek *tribos*, concerns the study of friction. Among specific areas included in this field are friction heat, friction noise, wear, lubrication, friction electrification, friction gas generation, and friction electron emissions.

Friction is deeply related to numerous phenomena in the natural world and to contact-surface technology in the industrial world. Accordingly, understanding the fundamentals of friction and methods of best harnessing it for practical use is important in developing industrial products, in improving their performance and securing their reliability, and in raising productivity.

With this in mind, the author has endeavored together with young researchers and students over the last 20 years to carry out research in the field of tribology and herein presents representative examples of the results of this research.

## 2. Micro-Mechanisms of Friction and Wear

### 2.1 Initiation and Propagation of Micro-Slip in Contact Interface

In **Fig. 1** (a), elastic deformation under load  $W$  results in formation of a circular contact surface. Friction force  $F$  is steadily increased on the lower spherical sample,

and accompanying the increase in  $F$  are increases in the sample's elastic deformation amount  $\delta$  and friction coefficient  $\mu = F/W$ .

Along with the increase in  $\mu$ , inside the circular contact surface the micro-slip indicated by the green area propagates from the circumferential region toward the center. Macro-slip occurs at the point this micro-slip has propagated throughout the contact surface area, and the  $\mu$  value ( $\mu_s = 0.85$ ) at that time becomes the static friction coefficient.

In **Fig. 1** (b), two point-defects exist in the circular contact surface's center area. In this case the micro-slip propagates from around these defects toward the circumference. At the same time, micro-slip also propagates from the circumferential region toward the center. Once these two propagations meet, macro-slip occurs, and the static friction coefficient becomes  $\mu_s = 0.69$ .

**Figure 2** shows micro-slip occurrence and propagation in four different types of contact surface configurations. Micro-slip covers the entire contact surface most quickly in the case of the triangle shape, displaying the lowest of the four values at  $\mu_s = 0.32$ .

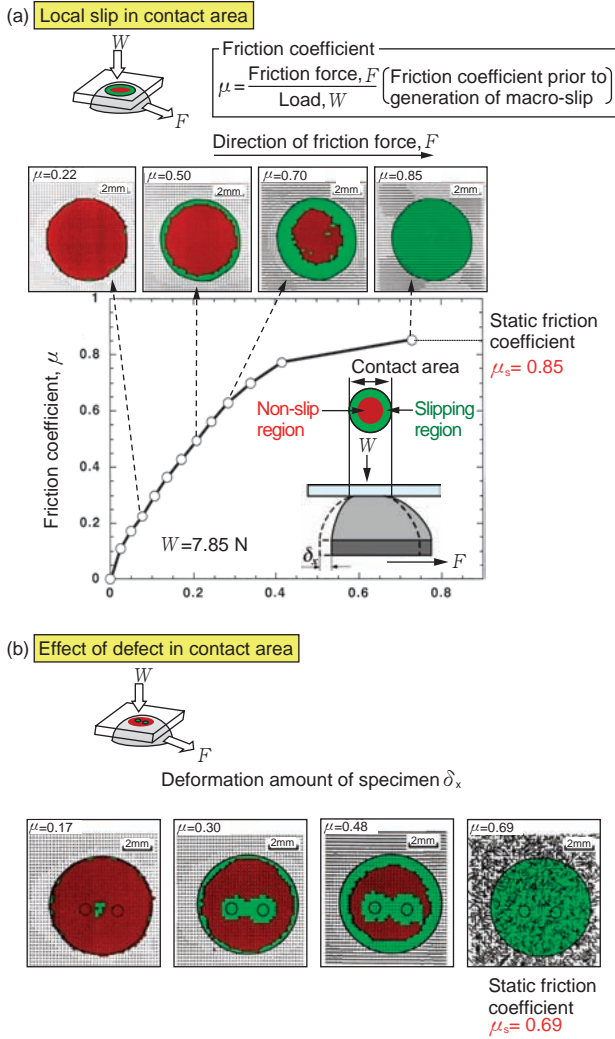


Fig. 1 Micro-slip in contact area corresponding to the increase in friction force and the static friction coefficient<sup>1)</sup>

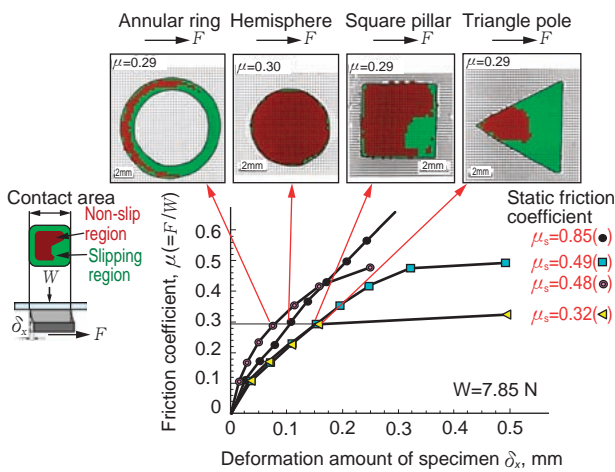


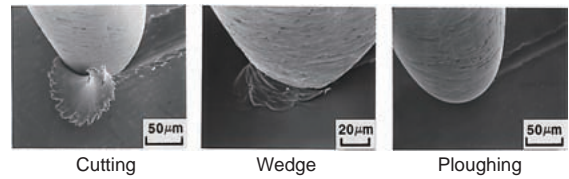
Fig. 2 Effect of shape of contact area on micro-slip and static friction coefficient<sup>1)</sup>

## 2. 2 Wear Map

Metals are subject to various types of wear such as abrasive wear, adhesive wear, fluid wear, fatigue wear and corrosive wear, and even in regard to the same wear type, they are subject to differing wear modes.

Figure 3 shows a wear map depicting, by the two parameters of penetration depth  $D_p$  and contact surface dimensionless shear strength  $f$ , the wear occurrence ranges for the cutting mode, wedge mode and ploughing mode, three modes of abrasive wear.

(a) SEM (scanning electron microscope) images of three wear modes



W: Load  
 F: Friction force  
 H: Hardness  
 R: Projection radius  
 a: contact circle radius  
 h: Engagement depth

$$D_p = \frac{h}{a} = R \left( \frac{\pi H}{2W} \right)^{\frac{1}{2}} - \left( \frac{\pi R^2 H}{2W} - 1 \right)$$

(b) Abrasive wear map of metal

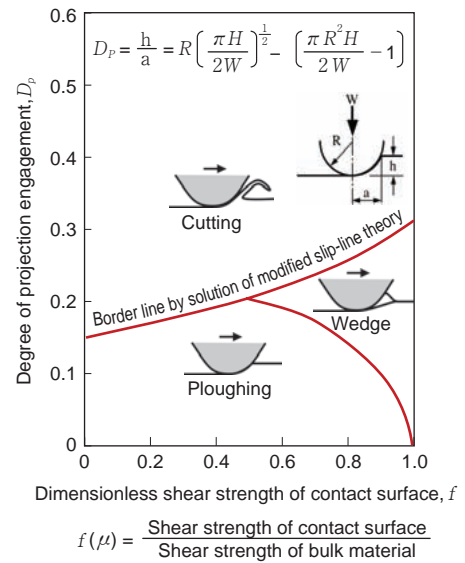
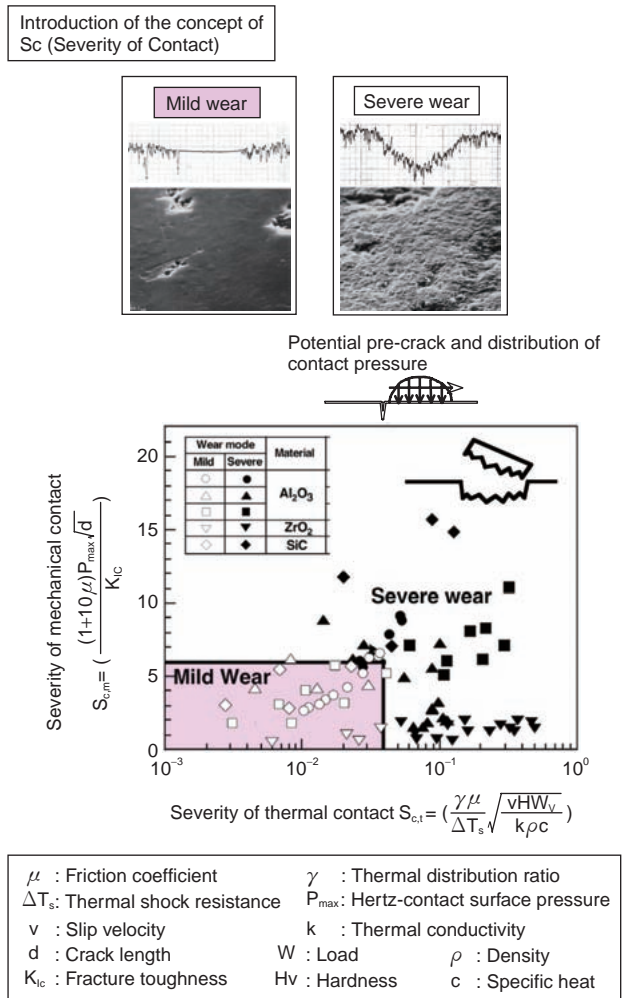


Fig. 3 Abrasive wear map of metals<sup>2)</sup>

**Figure 4** shows a wear map depicting, by mechanical contact severity  $S_{cm}$  and thermal contact severity  $S_{ct}$ , the occurrence ranges of mild wear (a smooth wear surface is formed) and severe wear (a coarse wear surface is formed) observed on identical ceramic types.

**Figure 5** shows a wear map depicting, by the coating and base material hardness ratio and the coating thickness and contact radius ratio, the occurrence range of three coating forms of delamination (delamination within the coating, delamination in the coating and base material interface, delamination within the base) occurring when a hard coating surface is subjected to repeated wear.



**Fig. 4** Wear map of ceramics describing mild and severe wear<sup>3)</sup>

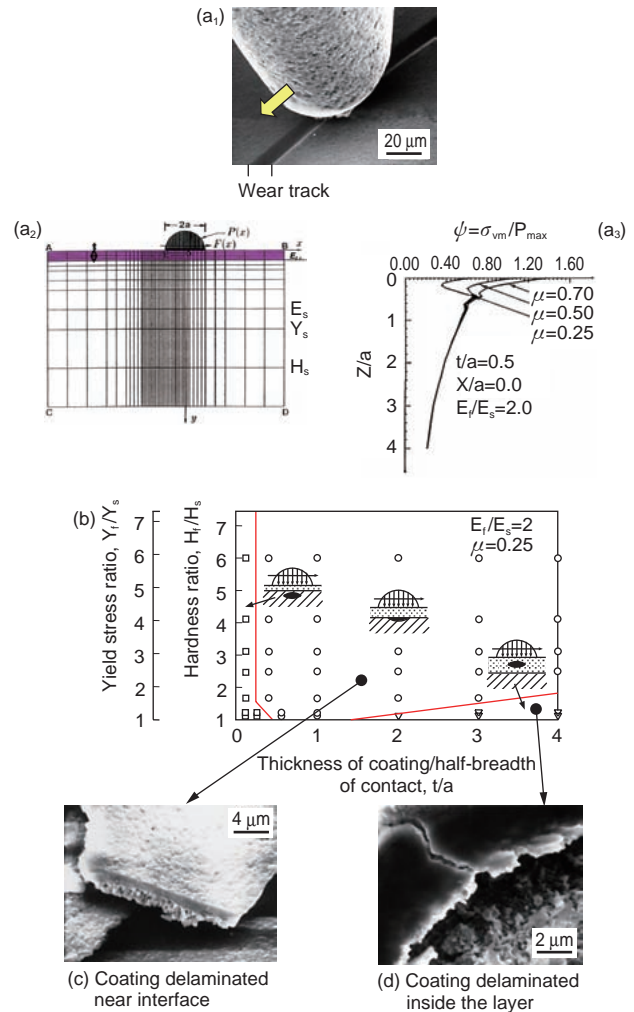


**Fig. 5** Wear map of delamination of hard coatings<sup>4),5)</sup>

### 2. 3 Simulation of Flow Wear

**Figure 6** shows thin filmy flow wear particles of steel in oil. **Figure 7** shows the results of continuous SEM observations of flow wear process on steel surface generated by friction cycles on a single surface area. By  $1.6 \times 10^4$  passes of repeated friction, it is understood that a single flow wear particle has been formed. **Figure 8** shows a Vickers indentation mark formed on a steel sliding surface that is covered by repeated flow of surface layer and gradually becomes smaller. When the change  $\Delta D_x$  of the mark size is measured, **Fig. 9** is obtained. From **Fig. 9**, the relation between surface flow rate  $R$  and contact pressure as shown in **Fig. 10** is obtained. In other words, it is understood that flow rate is sensitive to pressure and that flow wear occurs from surface flow around  $1 \text{ \AA}$ /pass.

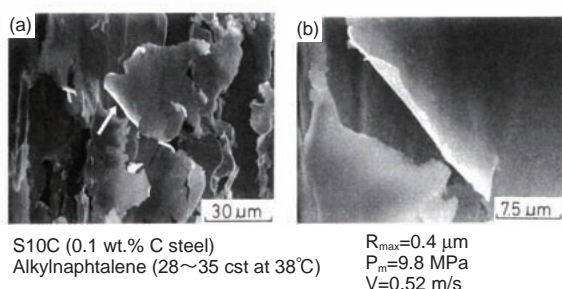


**Fig. 6** SEM images of flow wear particles of steel generated in oil<sup>6)</sup>

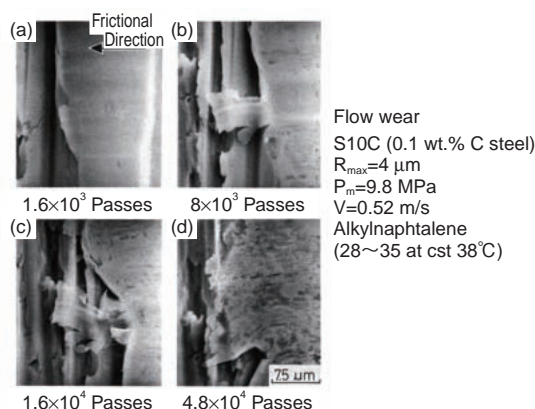


**Fig. 7** Generation process of a flow wear particle of steel by repeated friction<sup>6)</sup>

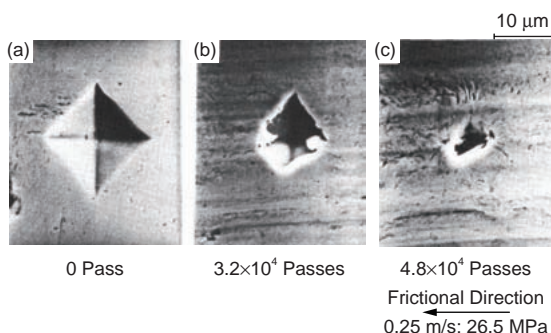


**Fig. 8** Simulation of flow wear process by the change of Vickers indentation mark in repeated friction<sup>7)</sup>

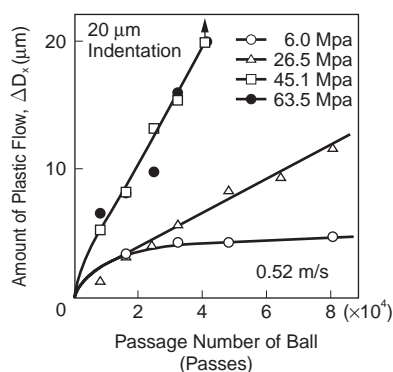


**Fig. 9** Relation between surface flow, number of friction passes and contact pressure<sup>7)</sup>

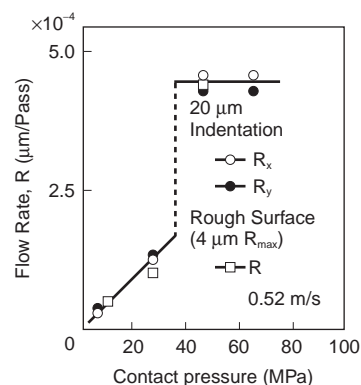
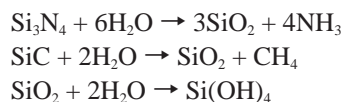


**Fig. 10** Relationship between surface flow rate and contact pressure<sup>7)</sup>

### 3. Water Lubrication of Ceramics

#### 3. 1 Generation of Low Friction by Running in Water

As shown in **Fig. 11**, when friction is generated repeatedly in water between SiC samples or Si<sub>3</sub>N<sub>4</sub> samples, the wear surfaces become smooth on a nanometer order. A 10 nm-order water film is formed by hydrodynamic effect, and the friction coefficient becomes less than 0.01. **Figure 12** shows wear surfaces so smooth that the sliding direction of pin and disk is not clear. It is considered that formation of these smooth surfaces is due to the occurrence on the contact surfaces of "tribo-chemical reactions" such as the following:



Even after eliminating water, wear surfaces such as these displayed low friction of  $\mu = 0.15$  over approximately  $10^4$  cycles.

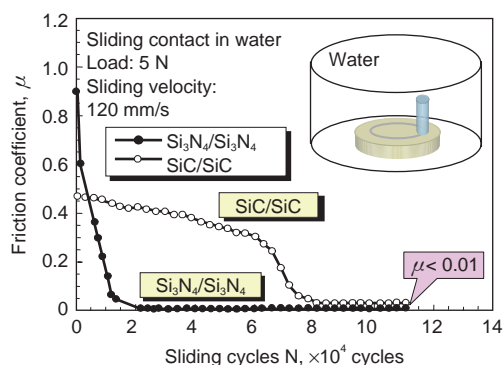


**Fig. 11** Reduction in friction coefficient of SiC/SiC and Si<sub>3</sub>N<sub>4</sub>/Si<sub>3</sub>N<sub>4</sub> by repeated friction in water<sup>8)</sup>

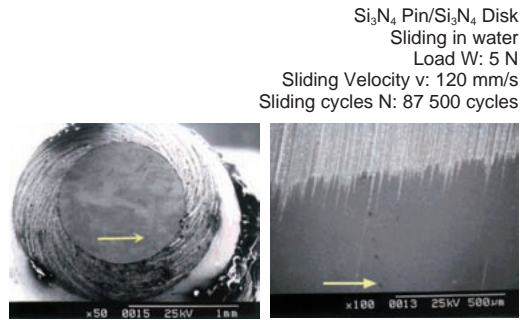


Fig. 12 Smooth wear surfaces on Si<sub>3</sub>N<sub>4</sub> pin and Si<sub>3</sub>N<sub>4</sub> disk formed by repeated friction in water<sup>9)</sup>

3. 2 Effect of Surface Texture on Lubrication

Figure 13 shows micro-pits formed on an SiC disk surface. If the size of these pits and the ratio of overall area they occupy is changed, the critical load value Wc obtained through seizure testing in water changes significantly, as shown in Fig. 14. Figure 15 shows the influence of pit depth/diameter h/d and area ratio r (%) on Wc. Wco is the Wc value in the case of no pits and is constant. From this figure, it is known that the Wc/Wco > 2.0 to 2.5 value exists in the range h/d = 0.01 to 0.02, r = 5%.

If the various pit patterns shown in Fig. 16 are formed, the changes in friction coefficient μ and critical load Wc become even greater by each pattern, as shown in Figs. 17 and 18. The value μ ≈ 0.0001 shown in Fig. 17 can contribute significantly to practical applications of water lubrication.

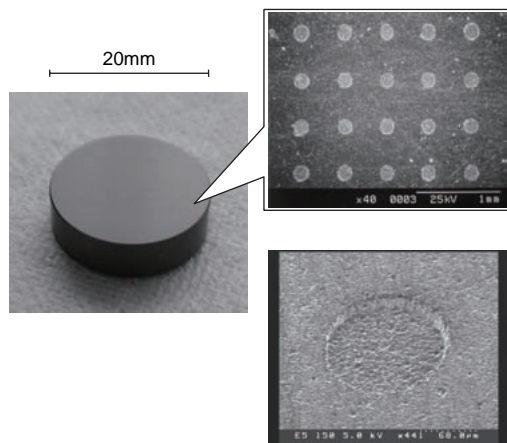


Fig. 13 Micro-pits formed on SiC disk surface<sup>10)</sup>  
Pit diameter: 150 μm  
Pit depth: 3 to 4 μm

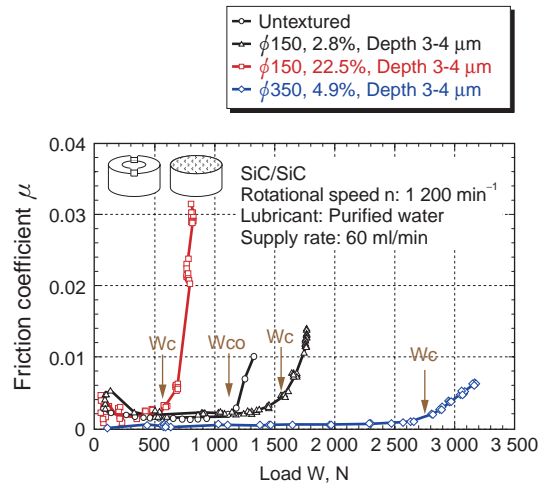


Fig. 14 Effect of size and area ratio of micro-pits on critical seizure load<sup>10)</sup>

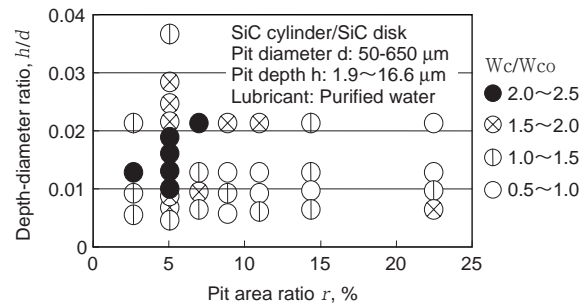


Fig. 15 Relationship among depth/diameter ratio h/d and area ratio r (%) of pits on disk surface and the normalized critical seizure load Wc/Wco<sup>10)</sup>

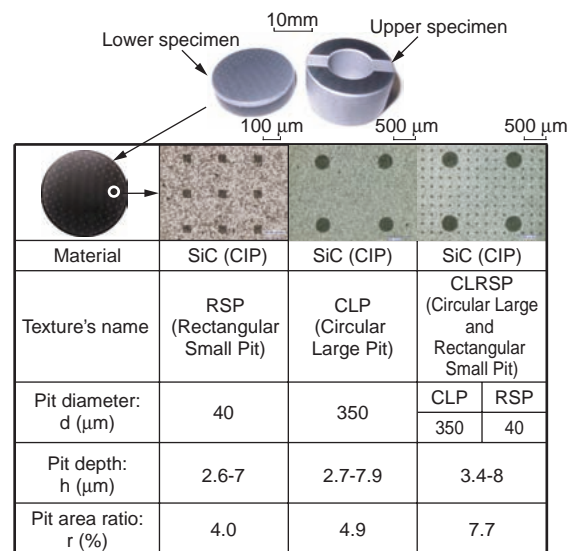
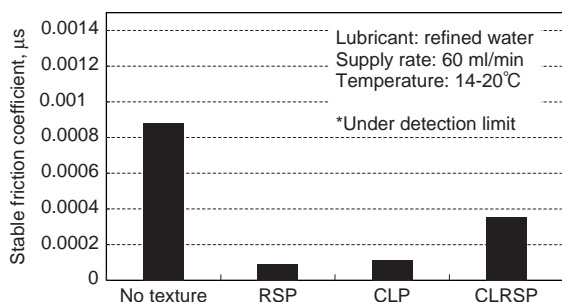
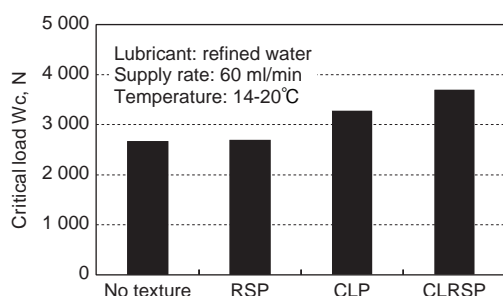


Fig. 16 Three pit patterns formed on SiC disk surface<sup>11)</sup>



**Fig. 17** Effect of three pit patterns on friction coefficients of SiC/SiC in water<sup>11)</sup>



**Fig. 18** Effect of three pit patterns on critical seizure load Wc of SiC/SiC in water<sup>11)</sup>

#### 4. Solid Film Lubrication in Vacuum

Ion plating or plasma coating is used to form solid film for lubrication in vacuum, and when usage has caused the film to wear to the point of disappearing, the system using that bearing stops. By "tribo-coating" to form a vapor-deposition coating immediately before and after sliding as shown in **Fig. 19**, a lubricant film can be supplied repeatedly at intervals as shown in **Fig. 20**. Moreover, the indium film formed by this tribo-coating can maintain a low friction coefficient much lower than that of conventional coatings for more than  $10^4$  cycles, as shown in **Fig. 21**.

It is important to note that these superior lubrication characteristics are obtained through the combination of  $\text{Si}_3\text{N}_4$  balls and SUS440C disks. **Figure 22** shows a TEM image of an indium tribo-layer formed by tribo-coating on an SUS440C disk sliding surface. The layer thickness is approximately 400 nm. The EDX analysis of **Fig. 23** shows a matrix comprising mainly the elements Si, Cr, and O. The black points distributed in the matrix are nano-particles whose main element is indium. The TEM image of **Fig. 24** shows the indium nano-particles to be crystalline phase and the matrix to be amorphous phase.

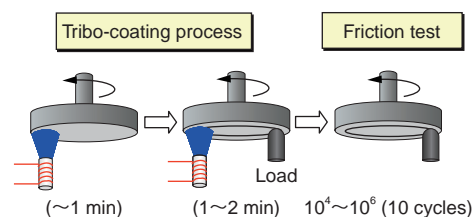


**Fig. 19** Friction assisted coating lubrication (Tribo-coating): Vapor-deposition of soft metal In for a few minutes just before and after initiation of sliding<sup>12)</sup>

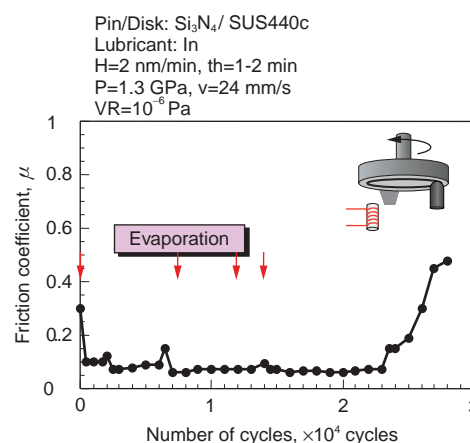


**Fig. 20** Effect of interval tribo-coating<sup>12)</sup>

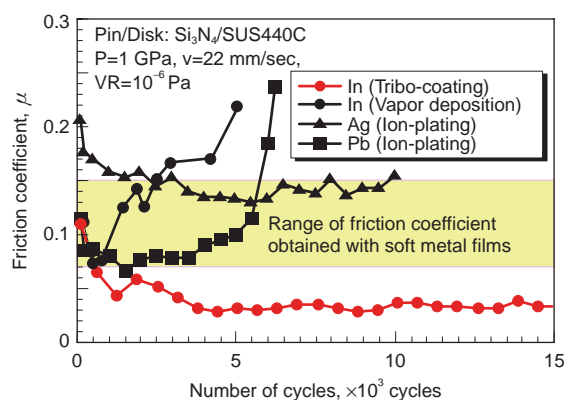


**Fig. 21** Lower friction and longer life of tribo-coating film in comparison with films by vapor-deposition and ion plating<sup>13)</sup>

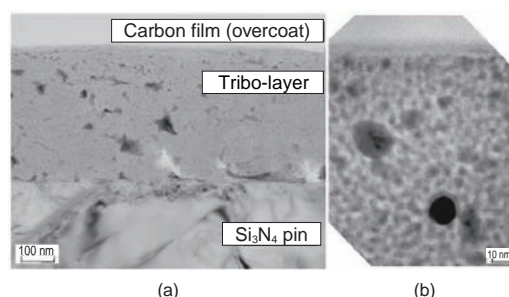
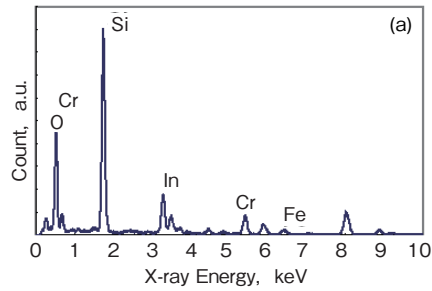
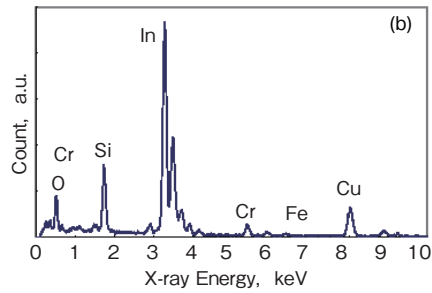


**Fig. 22** TEM image of tribo-layer on disk surface formed by tribo-coating of In<sup>14)</sup>



(a) Matrix in Fig. 22(a)



(b) Black points in Fig. 22(b)

**Fig. 23** Composition in tribo-layer on disk surface analyzed by EDX<sup>14)</sup>

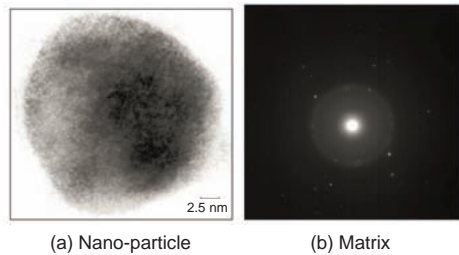


**Fig. 24** TEM image of tribo-layer<sup>14)</sup>

### 5. N<sub>2</sub> Gas Lubrication

Friction between a Si<sub>3</sub>N<sub>4</sub> ball and CN<sub>x</sub> coating varies dramatically depending on the gas environment. Of the seven gas environments shown in Figs. 25 and 26, only N<sub>2</sub> reduced the friction coefficient to less than 0.01. Figure 27 shows that by blowing N<sub>2</sub> gas on the contact surface in an air environment, a friction coefficient of around 0.7 is reduced very quickly to a level of 0.02.

The effectiveness of blowing gas on the contact surface in an air environment is observed as well in the case of blowing dry air or O<sub>2</sub>. Moreover, blowing N<sub>2</sub> on the surface after first blowing dry air or O<sub>2</sub> for 50 to 100 cycles significantly reduces the friction coefficient and wear ratio W<sub>s</sub>. Figure 28 shows that a value of μ ≈ 0.005 is obtained by blowing N<sub>2</sub> on a CN<sub>x</sub>/CN<sub>x</sub> surface in air after first blowing O<sub>2</sub> on the surface for 50 cycles. Figure 29 shows the μ and W<sub>s</sub> values after blowing various gas types on the contact surface. The observed values μ ≤ 0.05, μ ≤ 5 × 10<sup>-8</sup> mm<sup>3</sup>/N · m are very useful for practical applications.

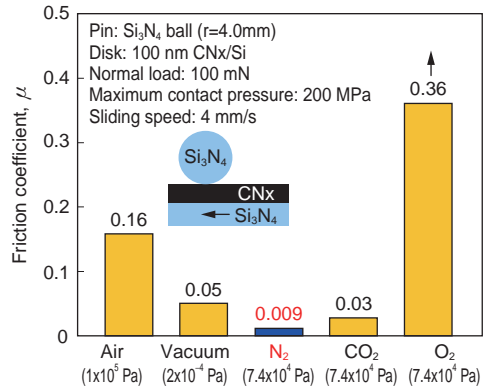


**Fig. 25** Effect of gas environment on friction of Si<sub>3</sub>N<sub>4</sub>/CN<sub>x</sub><sup>15)</sup>

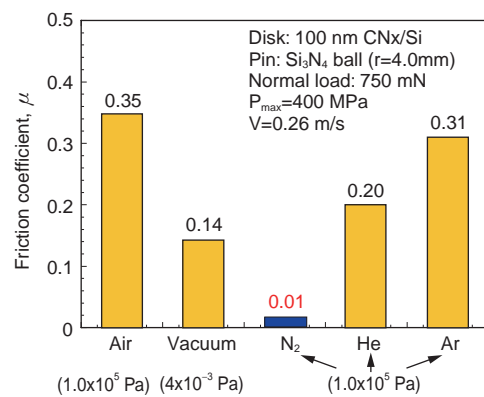


**Fig. 26** Effect of gas environment on friction of Si<sub>3</sub>N<sub>4</sub>/CN<sub>x</sub><sup>16)</sup>

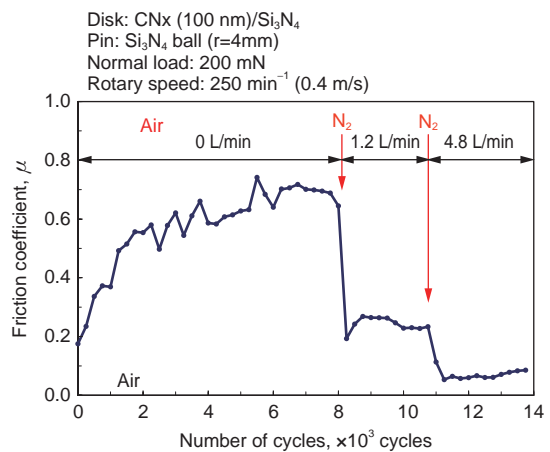


**Fig. 27** Effect of blowing N<sub>2</sub> gas to the contact on friction of Si<sub>3</sub>N<sub>4</sub>/CN<sub>x</sub> in air<sup>16)</sup>

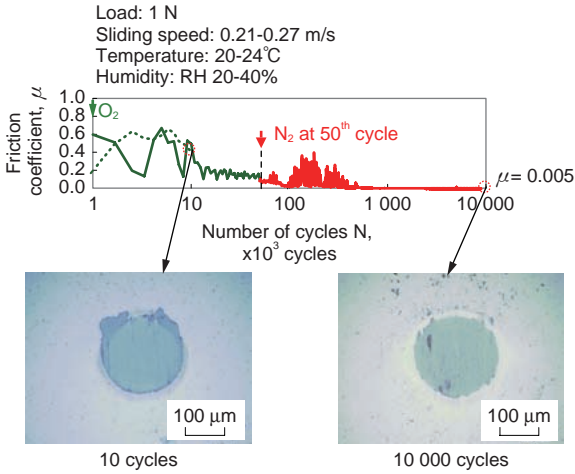


**Fig. 28** Change in friction coefficient of  $CN_x/CN_x$  by supplying  $N_2$  gas after initial 50 cycles in  $O_2$  gas<sup>17)</sup>

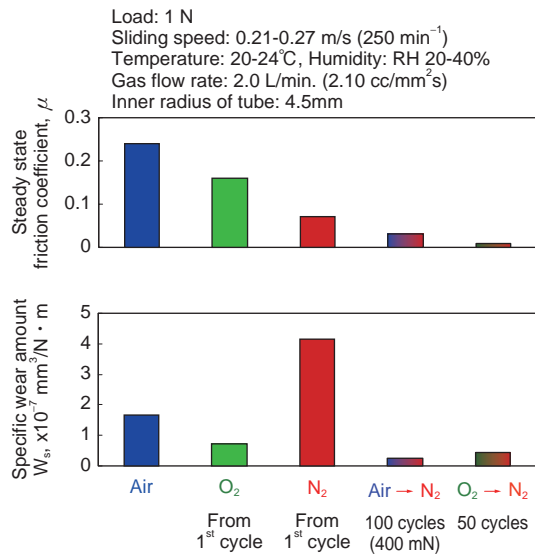
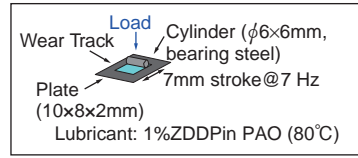


**Fig. 29** Values of friction coefficient  $\mu$  and wear ratio  $W_s$  ( $\text{mm}^3/\text{N} \cdot \text{m}$ ) at  $CN_x/CN_x$  in dry air,  $O_2$ ,  $N_2$  and combination of gases<sup>17)</sup>

## 6. Tribo-Chemical Reactions and Tribo-Layers

ZDDP (zinc dialkyl dithio phosphate) was invented in America and has been used for more than 60 years as an engine oil additive to improve wear resistance. When friction is repeated between a steel sheet on which an iron oxide film has been grown and a steel cylinder in PAO (Poly-Alpha Phosphate) oil containing ZDDP, the friction coefficient drops and a brownish friction surface is formed, as shown in **Fig. 30**. This surface is covered with a 200 nm tribo-layer as shown by the TEM image in **Fig. 31**. The main elements include Zn, Fe, P, C, S, O and Cr, which are distributed as shown by the EDX profile in **Fig. 31**. The mechanisms by which this microstructure



ZDDP: 4-methyl-2-pentanol

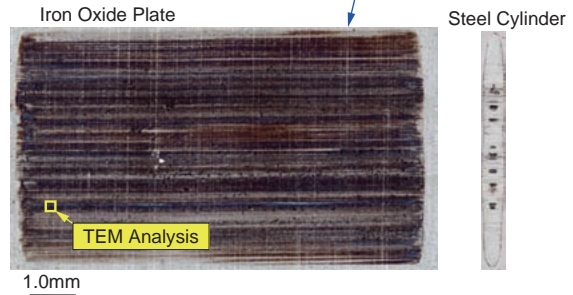
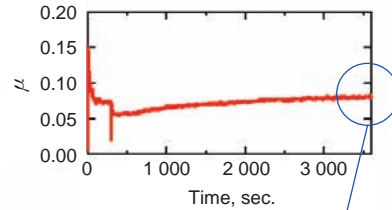
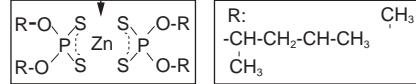
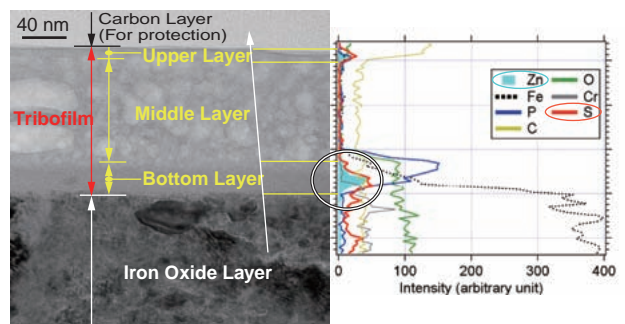
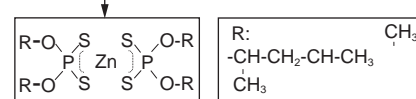


**Fig. 30** Outlook of surface layer on oxidized steel plate formed by friction against steel cylinder in oil (PAO) containing ZDDP<sup>18)</sup>

ZDDP: 4-methyl-2-pentanol



TEM Cross Section Photograph Near the Surface

**Fig. 31** TEM image of tribo-layer (to 400 nm) on friction surface of steel plate and depth profiles of elements by EDX<sup>18)</sup>

with layer thickness of 200 nm is formed and by which friction and wear are reduced are not clear. Certainly these mechanisms belong to the world of "tribo-chemical reactions" caused by the operation of friction.

### 7. Tribo-Applied Technology

**Figure 32** shows the shrink-fitting mechanism between lens and a tube adopted for laser printers in 1995. Here the shrink-fitter invented by Nitta and Kato was used, achieving a field of view 100 times larger than the conventional type. This is brought by contact micro-mechanisms as basic knowledge<sup>19)</sup>.

**Figure 33** shows a totally ceramic X-Y stage utilizing an ultrasonic motor for use in electron beam lithography in nonmagnetic vacuum environments. This stage was designed to have a drive pin and driven rail wear-resistant alumina, which are the key elements of ultrasonic motor, and was manufactured in 2000 by Kyocera. This is brought by wear mechanisms ceramics as basic knowledge<sup>20), 21)</sup>.

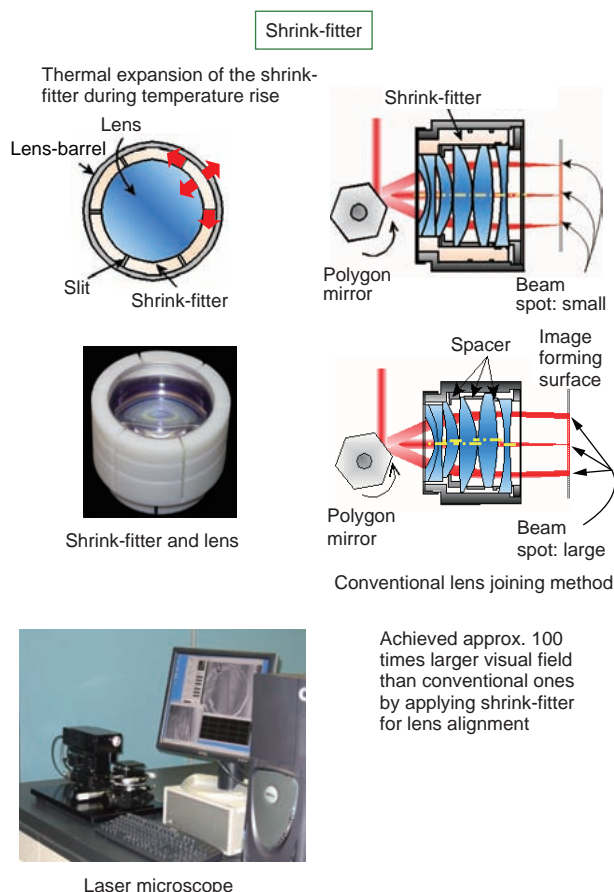


**Fig. 32** Laser microscope using shrink-fitter for ceramics polymer/metal shrink fitting

**Figure 34** shows the principle of magnetic fluid grinding, a method invented in 1990 enabling Si<sub>3</sub>N<sub>4</sub> ceramic balls to be grinded 40 to 100 times faster than by the conventional method with the same degree of roundness. The cost of magnetic fluid has not dropped, making this technology commercially unfeasible in terms of equipment investment and running costs. Wear mechanisms of Si<sub>3</sub>N<sub>4</sub> in water is the basic knowledge for the method<sup>22), 23)</sup>.

**Figure 35** shows a ball bearing currently being developed for space applications that has a built-in micro-heater and utilizes tribo-coating. The balls are Si<sub>3</sub>N<sub>4</sub>, and the races are SUS440C. As a result, knowledge concerning ceramic/metal optimal combinations and tribo-layers has become basic knowledge<sup>12), 13), 14)</sup>.

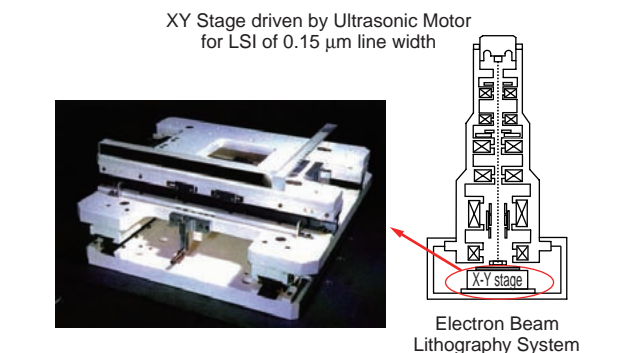


**Fig. 33** Totally ceramic X-Y stage driven by ultrasonic wave for electron beam lithography

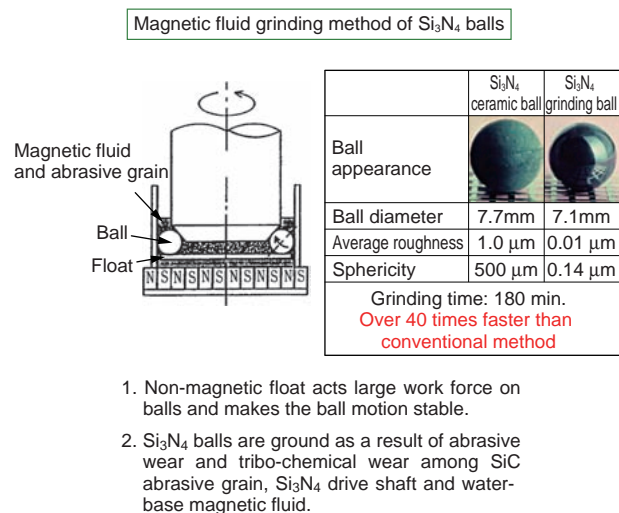


**Fig. 34** Magnetic fluid grinding of ceramic balls

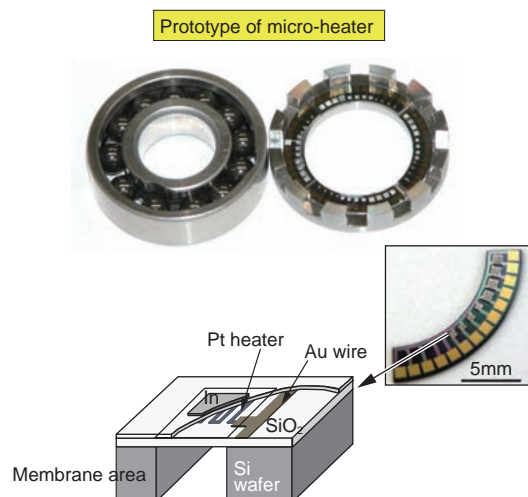


**Fig. 35** Ball bearing with micro-evaporators of in for space application

## 8. Conclusion

The life of technology supporting products tends to be short-lived. Put differently, such technology jumps forward dramatically every year. Attempting to survive by developing new products featuring little more than a changed appearance leads to weariness, a lack of uniqueness, little sense of responsibility for results, and frustration. Such an approach causes us to fall into an inescapable spiral and become little more than those humoring children with temporary novelty, as it were.

Development bringing dignity and true joy to those involved in "monozukuri" manufacturing is that which pioneers new technology and applications, improves performance (function and efficiency), reduces environmental load and cost, and calls to conscience of the mature consumer. It is the "high road" that gives one the satisfaction of having contributed to society and also leads to sure profitability. Pursuing profit by repeatedly developing new products intended mainly to excite consumers with superficial novelty while avoiding the rigor of advanced development is not the way of this road.

Many products of JTEKT can be considered to be on this high road. JTEKT has acquired much knowledge and basic experience related to tribology, and this certainly has contributed long-term to the significant improvement of performance and reliability and reduction of environmental load and cost in regard to these products.

The 35 figures provided in this paper show a sampling of the results the author obtained working mainly with a group of around 20 or 25 young researchers and students over the last 20 years. The fact that this small group of young people working without significant funding has been able to achieve such results in this short period of time attests to how deep, expansive, and relatively new

the field of tribology science and technology is.

It is thought that technology in the 21st century will be the key to determining the fate of our planet, and my hope is that JTEKT will play an important role in securing this technology. I would be delighted if this paper somehow contributed to that effort.

## Acknowledgement

In connection with the results presented herein, I wish to express my heartfelt thanks to Koyo Seiko and JTEKT for supporting our research efforts over the last 15 years related to  $\text{Si}_3\text{N}_4$  and  $\text{SiC}$  water lubrication,  $\text{Si}_3\text{N}_4/\text{SUS440C}$  indium lubrication, and  $\text{Si}_3\text{N}_4/\text{CN}_x$   $\text{N}_2$  gas lubrication mainly by providing ceramic balls and bearings.

## References

- 1) J. Liu, K. Oba, K. Kato and H. Inooka: Partial Slip Visualization at Contact Surface with the Correlation Method, Visualization Society of Japan, 15 (1995) 47-53.
- 2) K. Hokkirigawa and K. Kato: Abrasive Wear Diagram, Proceedings of Eurotrib'85, 4 (1985) 1-5.
- 3) K. Adachi, K. Kato and N. Chen: Wear Map of Ceramics, Wear 203/204 (1997) 291-301.
- 4) D. F. Diao, K. Kato and K. Hayashi: The Local Yield Map of Hard Coating under Sliding Contact, Thin Films in Tribology: Proceedings of the 19th Leeds-Lyon Symposium on Tribology, Leeds, UK, 1991, D. Dowson et al. (Editors), Tribology Series, 25 (1992) Elsevier, 419-427.
- 5) K. Kato: Microwear Mechanisms of Coatings, Surface and Coating Technology, 76-77 (1995), 469-474.
- 6) T. Akagaki and K. Kato: Plastic Flow Process of Surface Layers in Flow Wear under Boundary Lubricated Conditions, Wear, 117 (1987), 179-196.
- 7) T. Akagaki and K. Kato: Simulation of Flow Wear in Boundary Lubrication Using a Vickers Indentation Method, STLE Tribology Transactions, 31 (1988), 311-316.
- 8) M. Chen, K. Kato and K. Adachi: The Difference in Running-in Period and Friction Coefficient between Self-mated  $\text{Si}_3\text{N}_4$  and  $\text{SiC}$  under Water Lubrication, Tribology Letters, 11 (2001), 23-28.
- 9) M. Chen, K. Adachi and K. Kato: Friction and Wear of Self-mated  $\text{SiC}$  and  $\text{Si}_3\text{N}_4$  Sliding in Water, Wear, 250 (2001), 246-255.
- 10) X. Wang, K. Kato, K. Adachi and K. Aizawa: Loads Carrying Map for the Surface Texture Design of  $\text{SiC}$  Thrust Bearing Sliding in Water, Tribology International, 36 (2003), 189-197.

- 11) K. Adachi, K. Otsuka, X. Wang and K. Kato: Effects of Surface Texture on Water Lubrication Properties of Advanced Ceramics, *Journal of the Japan Society for Abrasive Technology*, 50 (2006), 107-110.
- 12) K. Kato, H. Furuyama and M. Mizumoto: The Fundamental Properties of Tribo-Coating Films in Ultra High Vacuum, *Proceedings of the Japan International Tribology Conference Nagoya, 1990*, 1 (1990), 261-266.
- 13) K. Adachi and K. Kato: Reliable Design of Space System in Tribology Viewpoint, *Proceedings of the 22nd International Symposium on Space Technology and Science*, 1, (2000), 593-598.
- 14) K. Adachi and K. Kato: In-situ and On-demand Lubrication by Tribo-coating for Space Applications, *Journal of Engineering Tribology, IMechE*, to be published.
- 15) N. Umehara, M. Tatsuo and K. Kato: Nitrogen Lubricated Sliding between CNx Coatings and Ceramic Balls, *Proceedings of the International Tribology Conference Nagasaki, 2000*, 2, (2001), 1007-1012.
- 16) K. Kato, N. Umehara and K. Adachi: Friction, Wear and N<sub>2</sub>-lubrication of Carbon Nitride Coatings: a Review, *Wear*, 254, (2003), 1062-1069
- 17) K. Adachi, T. Wakabayashi and K. Kato: The Effect of Sliding History on the Steady State Friction Coefficient between CNx-coating Under N<sub>2</sub> Lubrication, *Proceedings of the 31st Leeds-Lyon Symposium on Tribology, 2004*, Leeds, UK, D. Dowson et al. (Editors), *Tribology and Interface Engineering Series*, 48, Elsevier, (2005), 673-677.
- 18) K. Ito, J. M. Martin, C. Minfray and K. Kato: Formation Mechanism of a Low Friction ZDDP Tribofilm on Iron Oxide, *STLE Transactions*, 50, (2007), 1-6.
- 19) I. Nitta, K. Kigoshi and K. Kato: Study of the Fitting Strength between Ceramic and Metal Elements with the Use of a Shrink Fitter at Elevated Temperature (Proposal of the Shrink-Fit Method with the Use of a Shrink Fitter and Experimental Results), *JSME International Journal Series 3*, 32 (1989), 632-639.
- 20) T. Honda and K. Kato: The Influence of Ultrasonic Shape on Friction and Wear Properties in Ultrasonic Drive, *JaST*, 41 (1996), 178-184.
- 21) K. Adachi, K. Kato and Y. Sasatani: The Micromechanism of Friction Drive with Ultrasonic Wave, *Wear*, 194 (1996), 137-142.
- 22) N. Umehara and K. Kato: A Study on Magnetic Fluid Grinding (1st Report, the Effect of the Floating Pad on Removal Rate of Si<sub>3</sub>N<sub>4</sub> Balls), *Transactions of the JSME (C)*, 54 (1988), 1599-1604.
- 23) N. Umehara and K. Kato: Principles of Magnetic Fluid Grinding of Ceramic Balls, *J. Appl. Electromagnetics in Materials*, 1 (1990), 37-43.